

# Atomistic Simulation of Phonon-Assisted Tunneling in Bulk-like Esaki Diodes

Reto Rhyner, Mathieu Luisier, Andreas Schenk

Integrated Systems Laboratory, ETH Zurich, Gloriastr. 35, 8092 Zurich, Switzerland

e-mail: rhyner@iis.ee.ethz.ch

**Abstract**—To correctly describe band-to-band tunneling in semiconductor materials with an indirect band gap like silicon electron-phonon scattering must be taken into account. However, combining electron-phonon scattering and an atomistic full-band basis, as needed in nanoscale device simulations, is a real challenge from a computational and theoretical point of view. We have developed a quantum transport solver that can fulfill this requirement for realistic quantum well and nanowire structures. Transport in bulk-like tunneling diodes, the basic elements of tunneling FETs, for which several experimental data are available, could only be modeled ballistically so far. Hence, we present in this paper a first validation of electron-phonon interaction in an atomistic full-band basis for bulk-like structures by means of simulations of phonon-assisted band-to-band tunneling currents in Esaki diodes.

## I. INTRODUCTION

Power dissipation has become a critical issue to design integrated circuits, especially now that devices are entering the nanoelectronics era. Field-Effect-Transistors (FETs), as found in today's integrated circuits, need at least 60 mV gate voltage change to increase their current by one order of magnitude at room temperature. The 60 mV/dec limit is inherent to FETs. It does not allow to scale the supply voltage as rapidly as the FET dimensions, unless a decrease of the ON current or an increase of the OFF current is acceptable. Keeping a large supply voltage will lead to unmanageable power dissipation problems in the future. Hence, a drastic reduction of the power consumption of transistors will only be possible if new device concepts are introduced to replace the conventional FETs.

Band-to-band tunneling transistors (TFETs) on the contrary could exhibit sub-threshold slopes well below 60 mV/dec as a consequence of their cold instead of hot electron flows. Hence, TFETs are considered in academic and industry as the candidates with the highest potential for low power applications [1]. So far, no experimental TFET has reached the desired performance (high ON current with a steep sub-threshold slope and a

low supply voltage) [2]. Establishing first a modeling and simulation environment could be really useful to understand the physics, optimize the device performance, and be able to fully exploit the potential of TFETs.

Because such upcoming tunnel nanostructures do not operate in spite of quantum-mechanical effects, but because of them, more sophisticated transport models have to be developed. These models must go beyond the classical and semi-classical approximations. They should include an atomistic representation of the simulation domain, offer a full-band description of the semiconductor properties, and be capable of solving quantum transport in devices of realistic sizes. However, more evolved approaches cause a substantial increase of the computational burden especially if one includes electron-phonon scattering as required to correctly describe band-to-band tunneling in semiconductor materials with an indirect band gap like silicon, the material of reference in electronics. We already developed a tool that fulfills this requirement for realistic quantum well and nanowire structures [3]. Although the sizes of semiconductor devices have been aggressively scaled to the atomic range, realistic and recently fabricated Esaki diodes, the basic components of TFETs are still bulk-like, 1-D structures [4]. At the quantum mechanical level, electron transport in bulk-like tunneling diodes could only be modeled ballistically so far. Hence, we present in this paper a first validation of electron-phonon interactions in an atomistic full-band basis for bulk-like structures by means of simulations of phonon-assisted band-to-band tunneling currents in Esaki diodes as shown in Fig. 1.

## II. METHOD

The starting point is an existing full-band quantum transport simulator based on the nearest neighbor  $sp^3d^5s^*$  tight-binding method which can already perform either ballistic transport simulations in the NEGF or in the Wave Function formalism for 3-D, 2-D and 1-D nanostructures [5] (3-D=wire, 2-D=ultra-thin body, 1-D=bulk-like), or include electron-phonon scattering in the NEGF formalism for 3-D and 2-D nanostructures

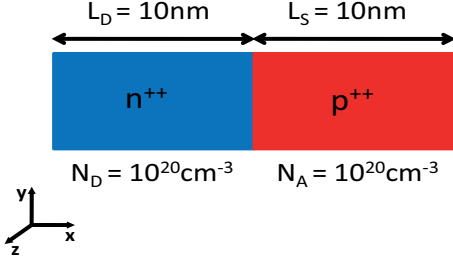


Fig. 1. Esaki diode structure composed of a 10nm heavily n-doped drain region and a 10nm heavily p-doped source region. The transport direction [100] is the  $x$  direction. The  $y, z$  directions are confined or periodically extended depending on what structure we are dealing with (1-D:  $y, z$  periodic, 2-D:  $y$  confined,  $z$  periodic, 3-D:  $y, z$  confined).

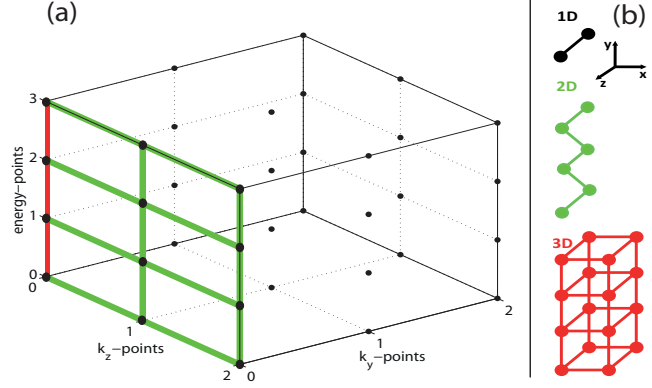


Fig. 2. Qualitative comparison of the electron-phonon coupling scheme in 1-D, 2-D, and 3-D structures. (a) Illustration of the exponential increase of the possible energy-momentum coupling induced by the electron-phonon scattering self-energies. In nanowires, only the energies situated along the red line are coupled. In ultra-thin bodies, all the momenta and energies situated in the same green plane are coupled. In bulk-like structures, all the energy and momentum points situated in the 3-D box are coupled. (b) Schematic view of 1-D, 2-D, and 3-D atomic unit cells.

[6], [3]. The simulator is extended here to treat electron-phonon scattering in the NEGF formalism for bulk-like structures, where the two directions ( $y, z$ ) perpendicular to the transport direction ( $x$ ) are assumed periodic. Hence, we have three spectral variables, the electron injection energy  $E$  into the device and the wave vectors ( $k_y, k_z$ ) which model the periodic dimensions. The scattering self-energies that account for the electron-phonon interaction are derived in the self-consistent Born approximation and have the following approximate form

$$\begin{aligned} \Sigma(E, k_y, k_z) &\approx \sum_{\omega_{ph}} \int_{-\pi}^{\pi} \frac{dq_y}{2\pi} \int_{-\pi}^{\pi} \frac{dq_z}{2\pi} \\ &\mathbf{V}(\omega_{ph}, q_y, q_z) \cdot \nabla \mathbf{H} \cdot (n_{ph}(\omega_{ph}) + \frac{1}{2} \mp \frac{1}{2}) \cdot \\ &\mathbf{G}(E \mp \hbar\omega_{ph}, k_y - q_y, k_z - q_z) \cdot \nabla \mathbf{H} \end{aligned}$$

The variable  $\mathbf{G}(E, k_y, k_z)$  is the Green's Function,  $\mathbf{V}(\omega_{ph}, q_y, q_z)$  represents a form factor,  $\nabla \mathbf{H}$  indicates the derivative of the nearest-neighbor tight-binding coupling matrix,  $\omega_{ph}$  is the phonon frequency, and  $n_{ph}(\omega_{ph})$  the corresponding Bose distribution. Since the full phonon band structure is taken into account, each electron energy  $E$  is coupled to several other energies  $E \mp \hbar\omega_{ph}$  (phonon emission/absorption) and all the momentum pairs ( $k_y, k_z$ ) are coupled to each other by the phonon momenta ( $q_y, q_z$ ). The 1-D energy-momentum coupling scheme is illustrated in Fig. 2 and compared to the 2-D and 3-D cases. While going from 3-D to 1-D structures, the computational complexity decreases due to a reduction of the number of atoms in the device

structure, but an exponential increase of the  $(E, k_y, k_z)$  coupling induced by electron-phonon scattering is simultaneously observed. This arising complexity increases the computational burden by orders of magnitude. Such a model therefore demands for an efficient implementation, a massive parallelization of the work load, and the usage of supercomputers to simulate realistic structures. Finally, once convergence between  $\Sigma(E, k_y, k_z)$  and  $\mathbf{G}(E, k_y, k_z)$  is reached, the carrier and current densities can be calculated in the NEGF/tight-binding formalism as

$$\begin{aligned} n(\mathbf{r}) &= -i \sum_j \int_{-\pi}^{\pi} \frac{dk_y}{2\pi} \int_{-\pi}^{\pi} \frac{dk_z}{2\pi} \int \frac{dE}{2\pi} \\ &\text{tr}(\mathbf{G}_{jj}^<(E, k_y, k_z)) \delta(\mathbf{r} - \mathbf{R}_j) \\ &\text{and} \\ J(\mathbf{r}) &= \frac{e}{2\hbar} \sum_{i_1, i_2} \int_{-\pi}^{\pi} \frac{dk_y}{2\pi} \int_{-\pi}^{\pi} \frac{dk_z}{2\pi} \int \frac{dE}{2\pi} \\ &\text{tr}(\mathbf{H}_{i_1, i_2} \cdot \mathbf{G}_{i_2, i_1}^<(E, k_y, k_z) \\ &- \mathbf{G}_{i_1, i_2}^<(E, k_y, k_z) \cdot \mathbf{H}_{i_2, i_1})(\mathbf{R}_{i_2} - \mathbf{R}_{i_1}) \delta(\mathbf{r} - \mathbf{R}_{i_1}), \end{aligned}$$

respectively. The charge density  $n(\mathbf{r})$  is used in the Poisson equation solved on a finite element grid to update the value of the electrostatic potential.

### III. RESULTS

We first consider the bulk-like (1-D) Si Esaki diode shown in Fig. 1 to validate our model. The transport

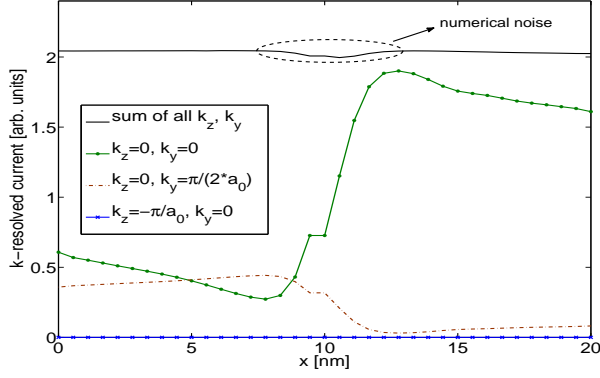


Fig. 3. Position-resolved dissipative current calculated for the 1-D structure in Fig. 1 at  $V_{ds} = -0.5V$ . The current is compared for different  $(k_z, k_y)$  components. The solid black line shows that the total current is conserved all along the Esaki-diode up to some numerical noise.

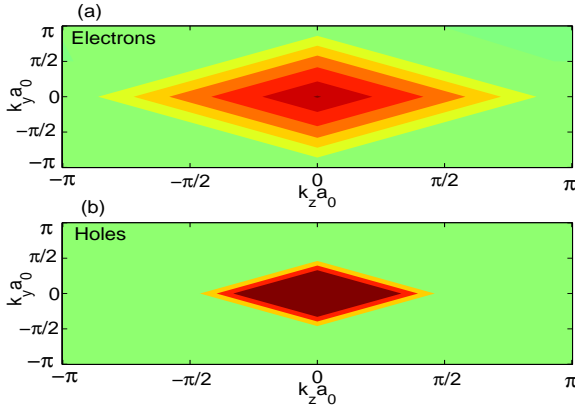


Fig. 5.  $(k_y, k_z)$ -resolved dissipative current calculated for the 1-D structure in Fig. 1 at  $V_{ds} = -0.5V$ . Dark red indicates high current concentrations, light green no current. (a) represents the beginning of the device (0nm), (b) represents the end of the device (20nm).

direction  $x$  is along the [100] crystal axis. To describe the periodically extended  $y$  and  $z$  directions a coarse  $(k_y, k_z)$  grid of  $5 \times 5$  points is used in this first investigations. As shown in Fig. 3, the total current remains constant from drain to source which is an important requirement in device simulations [7]. Since there are several thousands of different terms that must cancel each other to ensure current conservation, Fig. 3 is a good indication that the model implementation is correct.

An important feature of electron-phonon scattering is that it changes the spectral and spatial current distribution of a device, as depicted in Fig. 4 for two different  $(k_y, k_z)$  combinations. Due to electron-phonon interaction, electrons can be transferred from one  $(k_y, k_z)$  pair

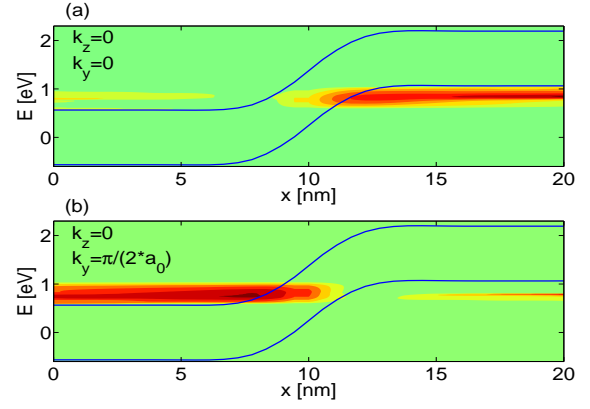


Fig. 4. Energy- and position-resolved dissipative current for the 1-D structure in Fig. 1 at  $V_{ds} = -0.5V$ . Dark red indicates high current concentrations, light green no current. The blue lines show the band edges. (a) and (b) represents two different  $(k_y, k_z)$  combinations.

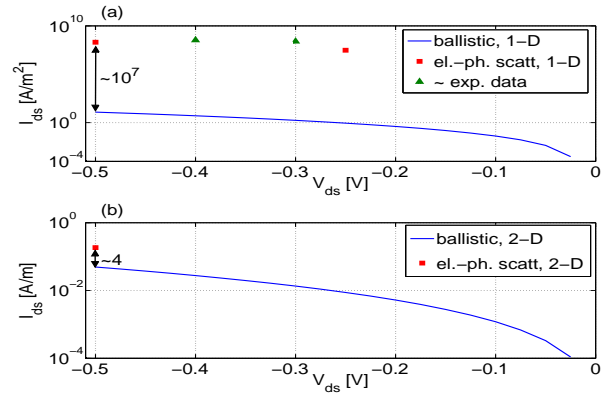


Fig. 6. (a): Comparison of the ballistic  $I_{ds} - V_{ds}$  curve against two points calculated with electron-phonon interaction and experimental data (b): Ultra-thin body structure with a confined width in  $y$  direction of 3nm. Comparison of the ballistic  $I_{ds} - V_{ds}$  curve against one current point calculated with electron-phonon interaction.

to the other and simultaneously gain or dissipate energy. For this reason, the current magnitude decreases from source ( $x=20\text{nm}$ ) to drain ( $x=0\text{nm}$ ) for  $(k_y = 0, k_z = 0)$  and increases from source to drain for  $(k_y = \frac{\pi}{2a_0}, k_z = 0)$ . Figure 5 shows the  $(k_y, k_z)$ -resolved current at the drain (0nm) and source (20nm). Due to electron-phonon interactions the current centered at the  $\Gamma$ -Point at the source spreads out in the drain conduction band. Figure 6 (a) demonstrates the need for including electron-phonon interaction to correctly describe the behavior of Si Esaki diodes. The phonon-assisted current is about 7 orders of magnitude larger than the ballistic one. Also, a comparison with experimental data [8] reveals that the current is already in the right order of magnitude even though

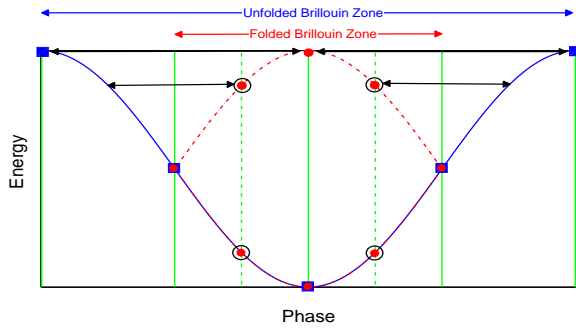


Fig. 7. Simple illustration in one dimension of the improved  $k$ -grid quality when supercells are used. Blue shows the bandstructure based on the primitive unit cell. The 5 solid blue squares correspond to 5  $k$ -points. Red shows the folded bandstructure based on a two times larger supercell. The 8 solid red circles correspond again to 5  $k$ -points. The 4 marked red circles indicate the automatic increase of the  $k$ -grid quality arising from the folding of the bandstructure. Hence, a resolution equivalent to 9  $k$ -points can be achieved by using a two times larger supercell and only 5  $k$ -points.

we are using a really coarse  $(k_y, k_z)$  resolution. Using a finer grid would eventually further increase the current. Note that including electron-phonon scattering in Esaki diodes is much more important in bulk-like structures than in ultra-thin bodies: Figure 6 (b) shows the ballistic and phonon-assisted tunneling current in an ultra-thin body (2-D) Esaki diode. The width of the confined  $y$  direction is 3nm and for the periodically extended  $z$  direction 21  $k_z$ -points are used. The other properties are the same as in the 1-D case. Electron-phonon scattering only increases the current by a factor 4.

#### IV. CONCLUSION

Phonon-assisted band-to-band tunneling currents in bulk-like silicon Esaki diodes have been modeled with a full-band atomistic device simulation tool. We have shown that the dissipative current is about 7 orders of magnitude larger than the ballistic current, demonstrating that electron-phonon interaction is essential to correctly describe bulk-like silicon Esaki diodes. Also, a comparison with experimental data reveals that the current is already in the right order of magnitude even though we have used a coarse  $(k_y, k_z)$  resolution. Nevertheless, future works will concentrate on improving the  $(k_y, k_z)$  grid quality, for example by using supercells that automatically couple different momentum points as qualitatively depicted in Fig. 7 and Fig. 8. Improving the grid quality by the combining supercells and a direct increase of the grid size should optimize the

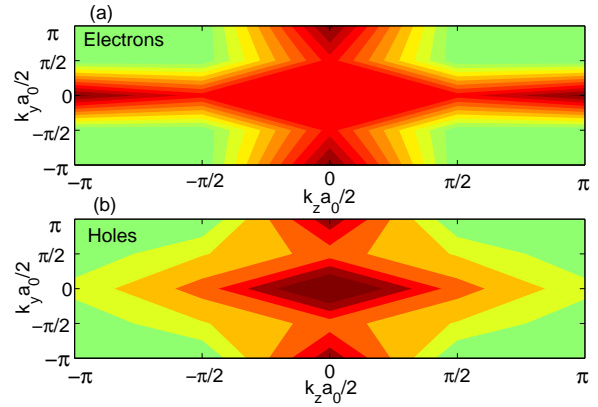


Fig. 8.  $(k_y, k_z)$ -resolved dissipative current calculated for the 1-D structure in Fig. 1 at  $V_{ds} = -0.5V$ . Same as in Fig. 5 but here we have extended the unit cell in  $y$  and  $z$  direction by factor of 2. As one can see in comparison with Fig. 5 the current is carried by more  $k$ -points which indicates more coupling between the  $k$ -points.

simulator performance and therefore help to reduce the computational burden.

#### ACKNOWLEDGMENT

This work was supported by SNF grant PP00P2\_133591, by the Swiss National Program Nano-Tera under the project Enabler, by a grant from the Swiss National Supercomputing Centre (CSCS) under projects ID s363 and s111, by NSF PetaApps grant number 0749140, by NSF through XSEDE resources provided by the National Institute for Computational Sciences (NICS). This research also used resources of the Oak Ridge Leadership Computing Facility at the Oak Ridge National Laboratory, which is supported by the Office of Science of the U.S. Department of Energy under Contract No. DE-AC05-00OR22725.

#### REFERENCES

- [1] Adrian M. Ionescu, Heike Riel, *Nature*, 479, 329-337, 2011.
- [2] A. C. Seabaugh and Q. Zhang, "Low voltage tunnel transistors for beyond CMOS logic", *Proc. IEEE* 98, 2095 (2010).
- [3] M. Luisier, *Proc. ACM/IEEE Conf. Supercomput.* 2010, pp. 1-11.
- [4] H. Schmid et al., *Nano Lett.*, 12(2), 699-703, 2012.
- [5] M. Luisier, G. Klimeck, A. Schenk, and W. Fichtner, *Phys. Rev. B*, 74, 205323, 2006.
- [6] M. Luisier, G. Klimeck, *Phys. Rev. B*, 80, 155430, 2009.
- [7] L. P. Kadanoff, G. Baym, "Quantum Statistical Mechanics", W. A. Benjamin Inc, New York (1962)
- [8] M. Oehme et al. *Appl. Phys. Lett.*, 95, 242109, 2009.